Earth and Planetary Science Letters, 48 (1980) 42–52

[2]

SEDIMENTARY BASIN FORMATION WITH FINITE EXTENSION RATES

GARY T. JARVIS

Department of Physics, University of Toronto, Toronto, Ont. M5S 1A7 (Canada)

and

DAN P. McKENZIE

Department of Earth Sciences, Madingley Rise, Madingley Road, Cambridge CB3 0EZ (England)

Received October 24, 1979
Revised version received March 10, 1980

Thinning of continental crust by rapid stretching of the lithosphere produces an initial subsidence and thermal anomaly. Wnen stretching ceases, slow decay of the thermal anomaly produces subsidence (due to thermal contraction) on a time scale of approximately 60 Ma. The dependence of the heat flow and subsidence histories on the rate of extension is determined here using a time-dependent analytical model. Results are compared with the predictions of a simpler instantaneous stretching model and constraints on the use of the latter are provided in terms of the duration and amount of stretching. For most basins the simple model gives reasonably accurate results provided the duration of stretching is less than 20 Ma.

1. Introduction

The problem of how sedimentary basins originate and develop has had a long and controversial history. A wide variety of models has been proposed, most of which have limited predictive power and require unobserved processes to operate in the crust and upper mantle. A major advance in this problem was Sleep's [1] demonstration that the subsidence of a number of basins was very similar to that of the ocean floor as it moves away from ridges. This observation suggested that sudden heating followed by conductive cooling of the lithosphere was in some way involved, but attempts [2,3] to produce a sudden temperature increase and to thin the continental crust at the same time were in disagreement with the widely accepted observation that the first event in the development of a basin was block faulting and subsidence, not elevation and erosion. Principally as a result of studies of heat flow, focal mechanisms and seismic refraction in the Aegean [4], McKenzie [5] proposed that the cause of both the thermal anomaly and of the thinning of the continental crust was an extensional event which stretched the lithosphere. This model took account of the difference between continental deformation, which is distributed, and oceanic deformation, which is principally confined to regions within 10 km of extensional plate boundaries. In this model the continental crust is thinned by a factor of β and the thermal anomaly is produced by passive upwelling of the hot asthenosphere. A sudden initial subsidence is associated with the crustal thinning. After the stretching event, heat is lost by vertical conduction and subsidence continues due to thermal contraction. Such a sequence of events can occur in any extensional environment. The principal difficulty with this model is the large values of the required extension, which must be taken up on listric normal faults. Though values of β of two have been reported from detailed studies of fault geometry in the Basin and Range region of the western U.S.A. [6], other studies of thin continental crust [7] have found insuf-

Contribution No. 21, Department of Earth Sciences.

ficient displacement on the faults to account for the observed continental thinning. Though this problem remains, the predicted relationship between the crustal thickness, subsidence and heat flow and the timing of the stretching event proposed in McKenzie [5] has now been confirmed in two basins. Sclater et al. [8] have looked in detail at the stratigraphy of the Pannonian Basin (Hungary), which appears to have been produced by extensional tectonics during the Miocene followed by rapid subsidence. With an average value of $\beta = 3$ the stretching model successfully accounts for the subsidence history, high heat flow, crustal thinning and the maturation of hydrocarbons at unusually shallow depths in the Pannonian Basin.

Christie and Sclater [9] have compared the subsidence history of the North Sea recorded in holes drilled west of the central graben with the crustal thickness obtained from seismic refraction. Both indicate extension by a factor of about 1.5. The success of the model in relating crustal thickness, subsidence and heat flow with one parameter, β, strongly suggests it is basically correct.

In McKenzie [5] it was assumed that stretching occurred instantaneously and therefore that the thermal anomaly was produced entirely by vertical advection, with no heat loss due to diffusion during extension. Provided the period of stretching is short compared to the relevant thermal time constant the conclusions drawn in that paper [5] are valid. However, when stretching occurs over a period comparable to the diffusion time scale some of the heat diffuses away before stretching is completed. The resultant thermal anomaly (and hence subsequent contraction) is thus reduced. In the case of very slow extension, no thermal anomaly is produced.

In this paper we investigate the effects of finite rates of extension on the heat flux and subsidence histories of sedimentary basins and provide constraints on the use of the simpler model given in McKenzie [5] (hereafter referred to as model 1).

2. Mathematical formulation

2.1. Physical model

We consider the two-dimensional physical model shown in Fig. 1. The lithosphere and crust are

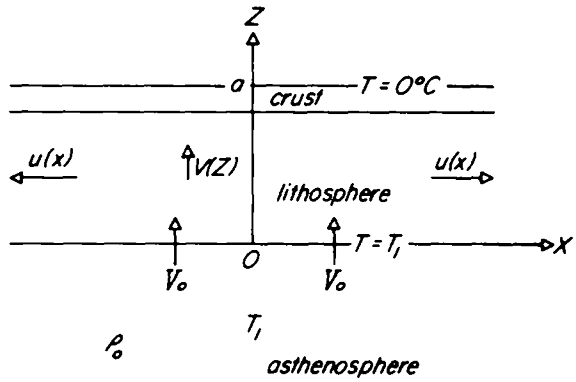

Fig. 1. Physical model for time-dependent stretching solution.

stretching with horizontal velocity $u(x)$, and asthenospheric material is flowing upwards across the plane $z = 0$ to replace the outflowing lithosphere. The upper surface, $z = a$, is maintained at $T = 0°C$ and the surface $z = 0$ is maintained at $T = T_1$ (the temperature of the asthenosphere below). For simplicity we deform the lithosphere in a pure shear strain field and let $v(x, 0) = V_0$, a constant, so that $\partial T/\partial x = 0$ at all times. (v is the vertical component of velocity; see Fig. 1.) Hence the origin can be chosen anywhere on the line $z = 0$. The vertical velocity vanishes at $z = a$ and is assumed to vary linearly with z:

$$v(z) = G(a - z) \tag{1}$$

where $G = V_0/a$ is the magnitude of the vertical velocity gradient across the depth a. The horizontal velocity vanishes at $x = 0$.

The relevant heat flow equation is:

$$\frac{\partial T}{\partial t} + G(a - z)\frac{\partial T}{\partial z} = \frac{\kappa \partial^2 T}{\partial z^2} \tag{2}$$

where T is temperature, t is time, and κ is the thermal diffusivity. Solving (2) allows us to follow the temporal development of the thermal anomaly.

The parameter G in equation (2) is related to the horizontal velocity through the continuity equation:

$$\frac{\partial u}{\partial x} = -\frac{\partial v}{\partial z} = G \tag{3}$$

Solving (3) for u gives:

$$u = Gx \tag{4}$$

G can also be related to β, the stretching factor introduced in McKenzie [5]. Since $u = \mathrm{d}x/\mathrm{d}t$, integrating (4) over a time interval Δt yields:

$$\frac{x}{x_0} = \mathrm{e}^{G\Delta t} \tag{5}$$

where $x_0 = x\ (\Delta t = 0)$, and since $x/x_0 = \beta$ we have:

$$\beta = \mathrm{e}^{G\Delta t} \tag{6}$$

Equation (6) relates β, G and the duration of stretching, Δt.

During the stretching phase there is an initial subsidence S_i due in part to the thinning of the low-density crust and in part to the thermal anomaly produced by the upwelling asthenosphere. For instantaneous stretching, as in model 1, assuming isostatic compensation both before and after stretching we have:

$$S_i = \frac{a\left[(\rho_0 - \rho_c)\dfrac{t_c}{a}\left(1 - \alpha T_1 \dfrac{t_c}{2a}\right) - \dfrac{\alpha T_1 \rho_0}{2}\right]\left(1 - \dfrac{1}{\beta}\right)}{[\rho_0(1 - \alpha T_1) - \rho_w]} \tag{7}$$

where ρ_0 and ρ_c are the densities of the lithosphere and crust, respectively, both at 0°C, ρ_w is the density of seawater. and t_c is the initial thickness of continental crust. When stretching occurs over a finite period of time, S_i is greater than that given by equation (7) due to the reduced thermal anomaly generated during the stretching. After stretching ceases diffusive decay of the thermal anomaly will produce a further subsidence S_t, a function of G, which approaches a final value S_G as $t \to \infty$. The total subsidence, achieved long after stretching has ceased, is S_{total} ($= S_i + S_G$) and depends only on the original crustal thickness t_c and the amount of stretching β. Assuming isostatic compensation throughout we have:

$$S_{\text{total}} = \frac{(\rho_0 - \rho_c)\, t_c}{[\rho_0(1 - \alpha T_1) - \rho_w]} \times \left[\left(1 - \frac{1}{\beta}\right) - \frac{\alpha T_1 t_c}{2a}\left(1 - \frac{1}{\beta^2}\right)\right] \tag{8}$$

In particular, if $t_c = 0$ (or $\rho_c = \rho_0$), then $S_{\text{total}} = 0$, and hence $S_i = -S_G$, where S_G is the total post-extensional subsidence. In section 2.3 below an explicit expression for S_G is given; thus S_i can be determined as a function of β, G and t_c as $S_i = S_{\text{total}} - S_G$.

2.2. *Temperature and heat flow during extension*

Equation (2) is solved using the technique of separation of variables. Substituting:

$$T(z, t) = \theta(z)\,\tau(t) \tag{9}$$

into (2) we have:

$$\frac{1}{\tau}\frac{\mathrm{d}\tau}{\mathrm{d}t} = \frac{\kappa}{\theta}\frac{\mathrm{d}^2\theta}{\mathrm{d}z^2} + \frac{G(z-a)}{\theta}\frac{\mathrm{d}\theta}{\mathrm{d}z} = -K\frac{\kappa}{a^2} \tag{10}$$

where K is a dimensionless constant. From (10) we have:

$$\tau = \tau_0 \exp(-Kt\kappa/a^2) \tag{11}$$

and:

$$\frac{\mathrm{d}^2\theta}{\mathrm{d}z^2} + \frac{G(z-a)}{\kappa}\frac{\mathrm{d}\theta}{\mathrm{d}z} + \frac{K\theta}{a^2} = 0 \tag{12}$$

Equation (12) poses an eigenvalue problem with nth eigenvalue K_n and corresponding eigenfunction θ_n. The complete solution $T(z, t)$ is obtained analytically, in the Appendix, as:

$$T(z, t) = \frac{-T_1 \operatorname{erf}[(z/a - 1)\sqrt{G'/2}]}{\operatorname{erf}\sqrt{G'/2}} + T_1 \sum_{n=1}^{\infty} a_n \theta_n \mathrm{e}^{-K_n \kappa t/a^2} \tag{13}$$

where a_n, the nth coefficient, is determined from the initial conditions (see Appendix), and $G' = a^2 G/\kappa$. The dimensionless parameter G' provides a relative measure of the velocities associated with advection and thermal diffusion. Hence for large values of G' we can expect the solution for T to reduce to that given by the simpler model in McKenzie [5]. From (13) we can see that a steady solution:

$$T_0(z) = \frac{-T_1 \operatorname{erf}[(z/a - 1)\sqrt{G'/2}]}{\operatorname{erf}\sqrt{G'/2}} \tag{14}$$

will be achieved after an infinite time (since the K_n are all positive – see Appendix). In the steady state a balance is maintained between the heat conducted and advected upwards and heat conducted across the upper surface. Consequently, the steady temperature solution is a function of the parameter G'. The summation in equation (13) represents a transient departure from the steady solution and decays with time.

The heat flux across the upper surface is:

$$F(t) = -k \left.\frac{\mathrm{d}T}{\mathrm{d}z}\right|_{z=a} \tag{15}$$

where k is the thermal conductivity. Evaluating the temperature gradient from (13), we have:

$$F(t) = \frac{kT_1}{a}\left\{\frac{\sqrt{2G'/\pi}}{\mathrm{erf}\sqrt{G'/2}} - a\sum_{n=1}^{\infty} a_n \exp(-K_n \kappa t/a^2)(d_z\theta_n)|_{z=a}\right\} \tag{16}$$

where $a(d_z\theta_n)|_{z=a}$ is determined in the Appendix.

2.3. Cooling and subsidence

At $t = \Delta t$ stretching ceases and diffusive cooling begins. The steady-state solution of (2) when $G = 0$ is:

$$T(z) = T_1(1 - z/a) \tag{17}$$

Hence during the cooling phase:

$$T(z, t) = T_1(1 - z/a) + T_1 \sum_{n=1}^{\infty} b_n \exp[-n^2\pi^2(t - \Delta t)\kappa/a^2] \sin n\pi z/a \tag{18}$$

where the coefficients b_n are given by:

$$b_n = \frac{2}{aT_1}\int_0^a [T(z, \Delta t) + T_1(z/a - 1)] \sin n\pi z/a \, \mathrm{d}z \tag{19}$$

The summation in equation (18) describes the transient temperature perturbation. The term $T(z, \Delta t)$ in (19) is given by equation (13) evaluated at $t = \Delta t$. In McKenzie [5] the initial temperature at the onset of cooling was specified analytically as:

$$\begin{aligned} T &= T_1, & 0 \leqslant z/a \leqslant (1 - 1/\beta) \\ &= T_1\beta(1 - z/a) & (1 - 1/\beta) \leqslant z/a \leqslant 1 \end{aligned} \tag{20}$$

and (19) was integrated to give:

$$b_n = \frac{2}{\pi}\frac{(-1)^{n+1}}{n}\left(\frac{\beta}{n\pi}\sin\frac{n\pi}{\beta}\right) \tag{21}$$

Substitution of (21) into (18) gives the equation used in McKenzie [5].

The surface heat flux during the cooling phase is given by a similar expression to (16). Differentiating (18) we have:

$$F(t) = \frac{kT_1}{a}\left\{1 + \pi\sum_{n=1}^{\infty} nb_n(-1)^{n+1} \times \exp[-n^2\pi^2(t - \Delta t)\kappa/a^2]\right\} \tag{22}$$

The subsidence due to thermal contraction is determined in terms of the elevation $e(t)$, at time t, measured relative to that as $t \to \infty$. Following an approach very similar to that of Parsons and Sclater [10], assuming isostatic equilibrium at the base of the old lithosphere and ignoring terms of order $(t_c/a)^2$ we have:

$$\begin{aligned} e(t) = {} & \frac{-a\alpha T_1}{[\rho_0(1 - \alpha T_1) - \rho_w + Bt_c/a]\,\pi} \\ & \times \sum_{n=1}^{\infty} \frac{b_n}{n} \exp[-n^2\pi^2\kappa(t - \Delta t)/a^2] \\ & \times \{\rho_0[1 - \cos n\pi(1 - t_c/a)] \\ & + \rho_c[\cos n\pi(1 - t_c/a) - (-1)^n]\} \end{aligned} \tag{23}$$

where:

$$B = \left[\rho_w\left(1 + \frac{\alpha T_1}{1 - \alpha T_1}\right)(1 - \rho_c/\rho_0) + (\rho_c - \rho_0)\right] \tag{24}$$

If there is no crust, that is if either $\rho_c = \rho_0$ or $t_c = 0$, then (23) reduces to:

$$\begin{aligned} e(t) = {} & \frac{-2a\rho_0\alpha T_1}{[\rho_0(1 - \alpha T_1) - \rho_w]\,\pi} \times \sum_{k=0}^{\infty} \frac{b_{2k+1}}{(2k + 1)} \\ & \times \exp[-(2k + 1)^2 \pi^2\kappa(t - \Delta t)/a^2] \end{aligned} \tag{25}$$

which to first order in αT_1 is the same as the equation given in McKenzie [5] but expressed here in a form consistent with (7) and (8).

The subsidence due to thermal contraction S_t is given by:

$$S_t = e(\Delta t) - e(t) \tag{26}$$

Since $e(t) \to 0$ as $t \to \infty$, the total post-extensional subsidence S_G is given by $e(\Delta t)$, or:

$$S_G = \frac{-a\alpha T_1}{[\rho_0(1-\alpha T_1) - \rho_w + Bt_c/a]\,\pi} \times \sum_{n=1}^{\infty} \frac{b_n}{n} \{\rho_0[1 - \cos n\pi(1 - t_c/a)] + \rho_c[\cos n\pi(1 - t_c/a) - (-1)^n]\} \quad (27)$$

or, when $t_c/a \ll 1$:

$$S_G \approx S_G^0 = \frac{-2a\alpha T_1\rho_0}{[\rho_0(1-\alpha T_1) - \rho_w]\,\pi} \sum_{n=1}^{\infty} (b_n/n) \quad (28)$$

where S_G^0 is the subsidence predicted when there is no crust. As discussed above (section 2.1), $S_G^0 = -S_i$ ($t_c = 0$) or:

$$S_G^0 = \frac{a\alpha T_1\rho_0(1 - 1/\beta)}{2[\rho_0(1-\alpha T_1) - \rho_w]} \quad (29)$$

Consequently, we may write:

$$S_{\text{total}} = S_i + S_G^0 + S_G' \quad (30)$$

where S_G' is the deviation from S_G^0 due to the presence of the crust. From (7), (8), (29) and (30):

$$S_G' = -\left[\frac{(\rho_0 - \rho_c)}{\rho_0}\left(\frac{t_c}{a}\right)^2 \frac{1}{\beta}\right] S_G^0 \quad (31)$$

Since S_G' is of order $(t_c/a)^2$ compared to S_G^0, for simplicity we have ignored S_G' and approximated S_G by S_G^0. The maximum error thus introduced into S_G is less than 3% and in many cases less than 1%, which is less than observational uncertainties.

3. Model calculations

In practice the infinite sums of the previous section are truncated after N terms where N is sufficiently large to ensure convergence. Due to the rapid decay of high-order modes (see Appendix) only the first few terms were generally required, although at the largest value of G' (=100) thirty terms were required in order to ensure convergence at times as small as 1 Ma.

Fig. 2 shows the evolution of the temperature distribution during stretching for a value of $G' = 50$.

TABLE 1
Values of physical parameters used (as in Parsons and Sclater [10])

a	= 125 km
ρ_0	= 3.33 g cm^{-3}
ρ_w	= 1.00 g cm^{-3}
α	= 3.28 × 10^{-5} °C^{-1}
T_1	= 1333°C
k	= 0.0075 cal °C^{-1} cm^{-1} s^{-1}
kT_1/a	= 0.8 cal cm^{-2} s^{-1}
κ	= 0.00804 cm^2 s^{-1}
a^2/κ	= 616 Ma
$\tau = a^2/(\pi^2\kappa)$	= 62.4 Ma

The steady-state profile given by (14) is reached at $t = \infty$. This same profile is obtained for all combinations of κ, a and G such that $G' = a^2G/\kappa = 50$. At $G' = 50$ the model has stretched by a factor of $\beta = 2$ after a time of:

$$\Delta t = (\ln\beta)/G = (\ln 2)/(\kappa G'/a^2) = 8.53 \text{ Ma} \quad (32)$$

The temperature profile calculated from equation (13) at this time is included in Fig. 2 and compared

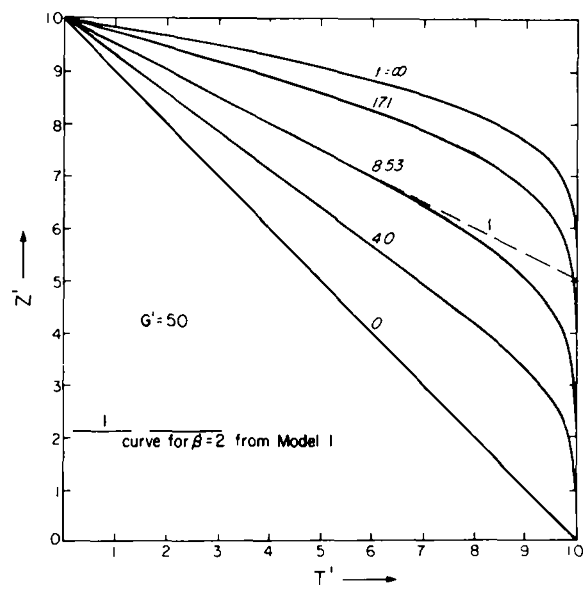

Fig. 2. Plots of dimensionless temperature $T' = T/T_1$ as a function of dimensionless height $z' = z/a$ for $G' = 50$. Each curve shows the temperature profile at a different time indicated in Ma since the onset of stretching. The broken line labelled 1 is from model 1 for $\beta = 2$. The profile labelled $t = 8.53$ corresponds to $\beta = 2$ in the present model.

to the simple curve assumed in McKenzie [5]. At this value of G' model 1 gives a reasonable approximation to the computed curve.

Fig. 3 shows a series of temperature profiles all computed for $\beta = 4$, but with different values of G'. As in Fig. 2 each profile shown is that which would occur for any combination of a, κ and G such that the ratio a^2G/κ has the value indicated. (Results presented in this manner are independent of changing estimates of individual physical parameters.) These profiles were computed from (13) at times given by $\Delta t = a^2(\ln 4)/\kappa G'$. The limiting case of $G' \to \infty$ corresponds to model 1. This figure demonstrates that for rapid stretching (large G') model 1 gives a good approximation to the thermal anomaly produced by stretching, while for slow stretching (small G') it greatly overestimates the magnitude of the anomaly.

If Δt, the duration of the stretching for a given basin, and β are known the mean value of G' can be determined as:

$$G' = \frac{a^2 \ln \beta}{\kappa\, \Delta t} \tag{33}$$

For the Pannonian Basin, for example, $\beta \simeq 3$ and $\Delta t \simeq 5$–10 Ma, giving $G' \simeq 120$–60. Since the stretched horizontal dimension of the basin is about 300 km the mean velocity between the two margins must have been between 20 and 40 mm/a, or comparable to that of slowly spreading ridges and to that now in progress in the northern Aegean [4]. Fig. 3 indicates that model 1 provides a good estimate of the thermal anomaly produced by stretching for this case.

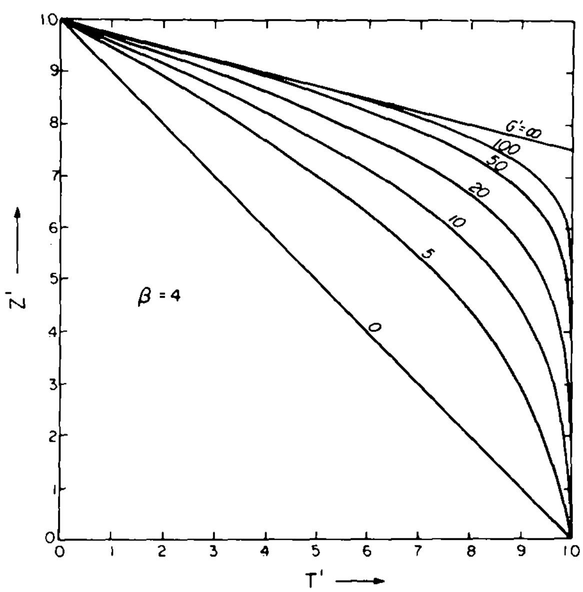

Fig. 3. Temperature profiles for $\beta = 4$ as computed with different values of G'. The case $G' = \infty$ corresponds to model 1.

4. Heat flow and subsidence compared to model 1

Fig. 4 shows the surface heat flux history as a function of G', for $\beta = 4$, and compares this with the history obtained from model 1 ($G' = \infty$). For small values of G' the surface heat flux at low values of $(t - \Delta t)$ is considerably less than predicted by model 1 and this discrepancy persists for times longer than the thermal time constant of the original plate.

Fig. 5 shows the dependence of the subsidence history after stretching has ceased on G', again for $\beta = 4$. The large range in post-extensional subsidence is due to the differing thermal anomalies produced at different values of G' (Fig. 3). The subsidence depends strongly on the rate of extension when $G' < 50$, but varies little when $G' \geqslant 50$.

In order to provide a quantitative measure of this dependence we have computed the ratio of the total post-extensional subsidence at a given value of G', S_G, to that predicted by model 1, S_∞. Graphs of S_G/S_∞ plotted as functions of G' are shown in Fig. 6a

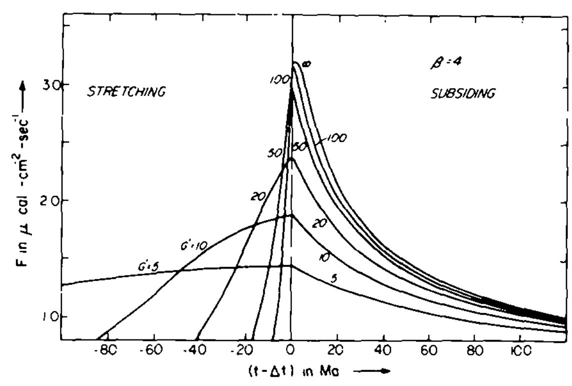

Fig. 4. Surface heat flux F as a function of time since the end of stretching $(t - \Delta t)$, for $\beta = 4$. The numbers on the curves indicate the corresponding values of G'. $G' = \infty$ corresponds to model 1. Negative values of $(t - \Delta t)$ indicate times before stretching ends.

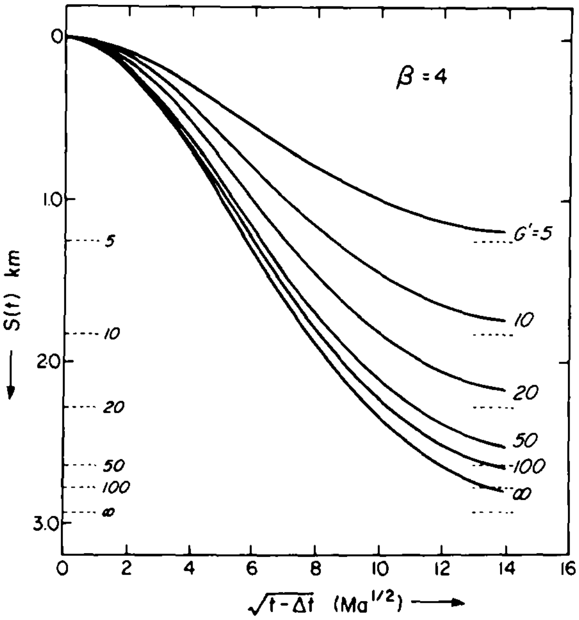

Fig. 5. Subsidence, S_t, of an empty basin shown as a function of the square root of time since stretching ceased $\sqrt{t - \Delta t}$ for $\beta = 4$ and different values of G' (t is measured in Ma). $G' = \infty$ corresponds to model 1.

for different values of β. For each β, the subsidence initially increases rapidly with G' and then asymptotically approaches S_∞ as G' increases. A rough estimate of the minimum value of G' above which the curves lie in the asymptotic range may be obtained from the thermal time constant of the depth below the stretched plate which has been heated to the asthenospheric temperature T_1. The depth of this zone is $a - a/\beta$ or $a(\beta - 1)/\beta$ and its thermal time constant is:

$$\tau' = \frac{a^2}{\pi^2 \kappa} \frac{(\beta - 1)^2}{\beta^2} = \tau \frac{(\beta - 1)^2}{\beta^2} \tag{34}$$

where τ is the time constant for the original plate of depth a. The other relevant time constant is that of the stretched plate:

$$\tau_s = \frac{a^2}{\pi^2 \kappa \beta^2} = \frac{\tau}{\beta^2} \tag{35}$$

(For $\beta < 2$, $\tau_s > \tau'$.) Substituting the larger of τ' and τ_s for Δt in equation (33) gives the corresponding minimum value of G'. Values of G' so computed are indicated in Fig. 6a by small arrows.

Although Fig. 6a is conceptually clear in terms of

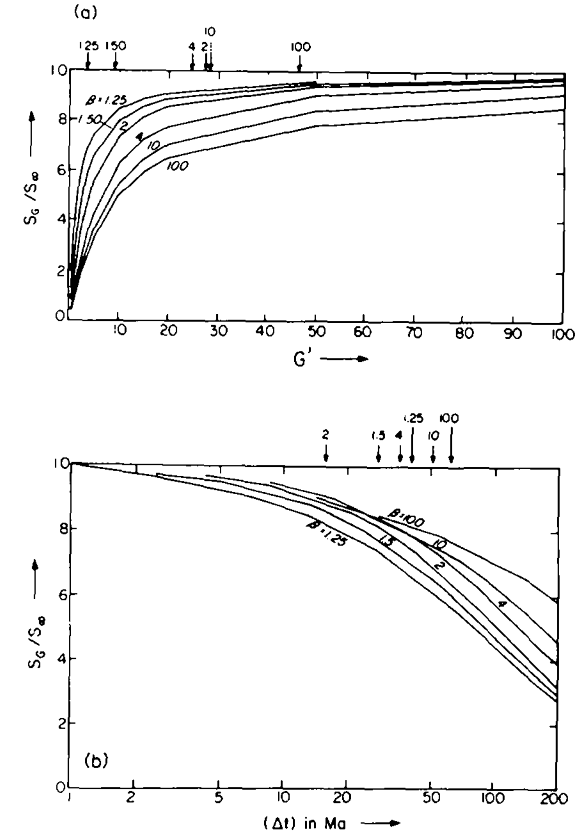

Fig. 6. (a) The ratio S_G/S_∞ plotted as a function of G' for different values of β. The small arrows indicate the estimate of the low end of the asymptotic range of each curve as determined from (34), or (35), and (33). The label on each arrow indicates the value of β. (Note: $S_G = e(\Delta t)_{G'}$.) (b) The ratio S_G/S_∞ plotted as a function of the duration of stretching Δt (in Ma), for different values of β. The numbers on each curve indicate the value of β for which the curve has been drawn. (Small arrows as in Fig. 6a.)

the present stretching model, it is geologically more useful to plot S_G/S_∞ vs. Δt, where Δt is the period over which stretching occurs. Such a graph is shown as Fig. 6b. For a given value of β, as the stretching period increases, G' must decrease and hence S_G/S_∞ decreases. The case of model 1 corresponds to $\Delta t = 0$ (instantaneous stretching) and $S_G/S_\infty = 1$. From Fig. 6b we can see that model 1 will predict the total subsidence correct to within 10% provided $\Delta t \leqslant 10$ Ma, and to within 20% provided $\Delta t \leqslant 20$ Ma. The exact value of Δt depends of course on β and may be almost twice as large as mentioned above in some cases (see Fig. 6b).

Unlike the subsidence the heat flow is controlled by the thermal structure of the stretched plate for all values of β. When stretching ceases, cooling is most rapid in the vicinity of the knee in the temperature profile at the base of the stretched plate. The surface heat flow will only be significantly affected after conductive cooling has propagated upwards and downwards from the base of the stretched plate for a distance a/β. The thermal time constant for a depth of

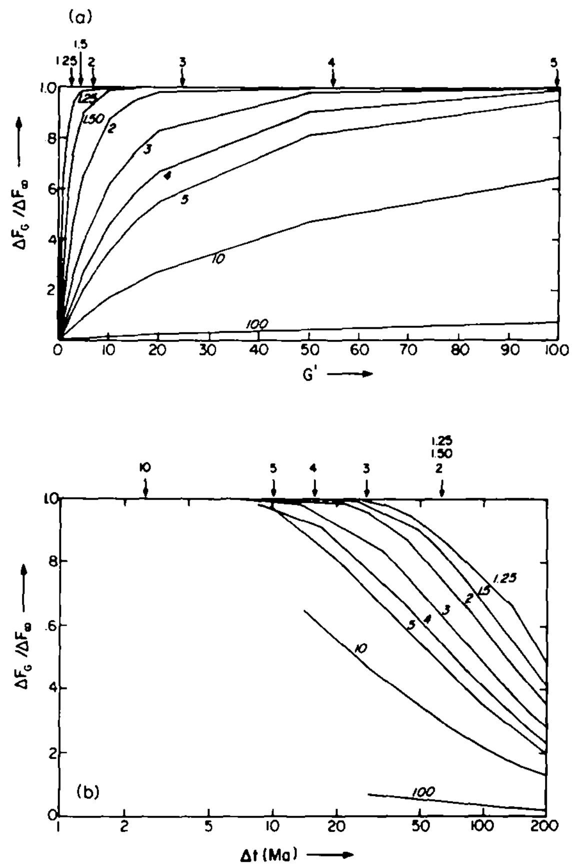

Fig. 7. (a) The ratio $\Delta F_G/\Delta F_\infty$ plotted as a function of G' for different values of β. The small arrows indicate the estimate of the low end of the asymptotic range of each curve as determined from (36) and (33). The label on each arrow indicates the values of β. (Note: $\Delta F_G = F(\Delta t)_G - F(\infty)$.) (b) The ratio $\Delta F_G/\Delta F_\infty$ plotted as a function of the duration of stretching Δt (in Ma), for different values of β. The numbers on each curve indicate the value of β for which the curve has been drawn. (Small arrows as in Fig. 7a.)

$2a/\beta$ is:

$$\tau'' = \frac{4a^2}{\pi^2 \kappa \beta^2} = 4\tau_s \qquad (36)$$

(For $\beta < 2$ the relevant time constant is that for the original plate of thickness a.) Hence model 1 will only give reliable estimates for the heat flow when the time during which stretching occurs is short compared with τ''. Fig. 7a shows the ratio of ΔF_G, the increase in heat flow when stretching stops, to ΔF_∞, that predicted by model 1, as a function G' with arrows to indicate the values of G' obtained from (36) and (33). The curve for $\beta = 4$ is constructed from the intercepts of F_G at the $(t - \Delta t) = 0$ axis of Fig. 4. Similarly the other curves summarize the convergence of ΔF_G to ΔF_∞, at $t = \Delta t$, for different values of β. At $\beta = 2$, for example, the convergence is a much more rapid function of G' than that shown in Fig. 4. Plotting $\Delta F_G/\Delta F_\infty$ against the time taken to produce the stretching (Fig. 7b) shows that the surface heat flow is more sensitive to β and the stretching rate than is the subsidence.

5. Discussion

The model proposed previously [5] is an idealization of continental stretching, since it takes no account of magmatic events, the lateral variation in extension and of the time taken to carry out the stretching. Of these problems the importance of the first is speculative. It appears unlikely that more than about 6 km of magma can be added to the thickness of the crust, even as $\beta \to \infty$, since this is the thickness of the oceanic crust. This argument was used in McKenzie [5] and has been supported by Sclater et al.'s [8] study of the Pannonian Basin. Whether lateral variations in β are important depends on whether the lithosphere behaves as an elastic plate or whether the faults on which the extension occurred continue to move during subsidence. The best approach to this problem is to compare simple calculations obtained from model 1 with observations in regions, such as continental margins, where the value of β varies rapidly. In this paper we have allowed the extension to occur in a finite time. In contrast to the other effects, the detailed tectonic history of many sedimentary basins has been determined from seismic reflection and drilling, and hence limits can be placed on the duration of the stretching event. Though it is not yet possible to obtain the extension rate from the history of fault movement, principally because the fault displacements can rarely account for the required extension, it is generally clear how long the major event lasted. The detailed calculations above refer to a particular two-dimensional extensional strain field, pure shear, with a constant strain rate, but the results are unlikely to be very different for more complicated three dimensional strain field provided the duration of the event is the same and β is obtained from the change in the crustal thickness. As in McKenzie [5] we have computed the subsidence of an empty basin and ignored the second-order effects of sediments on the thermal structure of the lithosphere. In order to obtain the thermal subsidence from observations of the depths to sediment horizons, the effects of sediment loading must be removed in accord with the stratigraphic record [8,11,12].

The principal result of this study is that the simple model proposed previously [5], in which the extension is instantaneous, gives results which differ little from the true behaviour provided the time taken to extend by a factor β is less than $60/\beta^2$ Ma. This condition which applies to both heat flow and subsidence is over-restrictive in most cases. If only the subsidence is of concern, then the time must be shorter than about $60/\beta^2$ Ma if $\beta \leqslant 2$ or $60(1-1/\beta)^2$ Ma if $\beta \geqslant 2$. If only the heat flow is of interest then the time must be shorter than about 60 Ma if $\beta \leqslant 2$ or $60(2/\beta)^2$ Ma if $\beta \geqslant 2$. Thus for $\beta < 3$ the heat flow predicted by model 1 is more reliable at a given time than is the subsidence, while for $\beta > 3$ the subsidence is more reliably predicted than is the heat flow. In the case of the Pannonian Basin, $\beta \simeq 3$ [8] and the above criteria indicate that the duration of stretching should be less than about 28 Ma for both subsidence and heat flow. Since the stretching event in the Pannonian Basin occurred over a period of less than 10 Ma [8] both the heat flow and subsidence should differ little from those obtained from model 1. In contrast the North Sea has extended less and over a period of perhaps as much as 50 Ma. Christie and Sclater [9] estimate that $\beta \simeq 1.5$, hence a time constant of 28 Ma for the subsidence and 60 Ma for the heat flow. Whether this difference strongly affects the subsidence after the extension ceased in the Early Tertiary depends on the stretching history. If it does the subsidence should be somewhat less than that predicted from model 1 (though Fig. 6b shows that even periods of stretching lasting as long as 90 Ma reduce the thermal subsidence by less than 50% when $\beta > 1.5$). In contrast, Fig. 7b shows that the heat flow is only slightly reduced for $\beta = 1.5$ and hence model 1 provides a rough estimate of β for the North Sea.

This investigation shows that the duration of extension of many sedimentary basins is likely to be sufficiently short for the instantaneous stretching model to be used to calculate the subsidence history. For $\beta > 3$, heat flow is more sensitive to the history of the extension, and care should be taken that the extension is sufficiently rapid before using the heat flow to estimate β. Nevertheless, the extension in both the Aegean and Pannonian Basins has probably been rapid enough for the errors in the instantaneous model to be less than observational errors.

Acknowledgements

We would like to thank J. Sclater and P. Christie for several helpful discussions on the Pannonian Basin and the North Sea. We also thank D. Yuen and W.R. Peltier for helpful comments on the mathematical development. One of us (G.T.J.) was supported during this work by a National Research Council of Canada Post-doctoral Fellowship. W.R. Peltier generously provided computing funds.

Appendix. Analytic solution of the temperature equation during stretching

Scaling all variables in terms of characteristic values we write:

$$z = az', \quad T = T_1 T', \; t = \frac{a^2}{\kappa} t' \quad \text{and} \quad G = \frac{\kappa}{a^2} G' \tag{A-1}$$

where the primed variables are dimensionless. Substituting (A-1) into equations (11) and (12) yields:

$$\tau = \tau_0 \exp(-Kt') \tag{A-2}$$

and:

$$\frac{d^2\theta}{dz'^2} + G'(z' - 1)\frac{d\theta}{dz'} + K\theta = 0 \qquad \text{(A-3)}$$

The solution of (A-3) is an eigenvalue problem with nth eigenvalue K_n and corresponding eigenfunction θ_n. This equation may be written in canonical form as:

$$\frac{d}{dz'}\left\{\exp[(z' - 1)^2 G'/2]\frac{d\theta_n}{dz'}\right\} + \exp[(z' - 1)^2 G'/2] K_n\theta_n = 0 \qquad \text{(A-4)}$$

Since equation (A-4) is of the Sturm-Liouville type, the eigenvalues K_n are real and the eigenfunctions θ_n are orthogonal with respect to the weighting factor $\exp[(z' - 1)^2 G'/2]$. That is:

$$\int_0^1 \theta_n\theta_m \exp[(z' - 1)^2 G'/2]\, dz' = 0 \text{ for } m \neq n \qquad \text{(A-5)}$$

From (A-2) we can see that provided K_n are positive, a steady solution will be achieved after an infinite time. The steady-state solution can be obtained by solving (A-2) and (A-4) with $K_n = 0$. Thus from (A-2):

$$\tau = \tau_0 \text{, say } \tau_0 = 1 \text{ ,} \qquad \text{(A-6)}$$

and from (A-4):

$$\exp[(z' - 1)^2 G'/2]\frac{d\theta_0}{dz'} = C \qquad \text{(A-7)}$$

where the subscript 0 indicates the steady-state solution and C is a constant determined by the boundary conditions. Solving (A-7) for θ_0 gives:

$$T_0'(z') = \tau_0\theta_0(z') = \frac{-\mathrm{erf}[(z' - 1)\sqrt{G'/2}]}{\mathrm{erf}\sqrt{G'/2}} \qquad \text{(A-8)}$$

The full time-dependent solution is given by the sum of the steady-state solution and a transient solution which decays with time:

$$T'(z', t') = T_0'(z') + T_1'(z', t') \qquad \text{(A-9)}$$

$T_1'(z', t')$ is determined from (A-2) and (A-3) with $K \neq 0$ and boundary conditions $\theta = 0$ on $z' = 0$ and 1.

Eigenvalues K_n and corresponding eigenfunctions θ_n are computed using the propagator matrix technique [13]. We define a two-component vector f as:

$$f = (\theta, d_z\theta) \qquad \text{(A-10)}$$

in terms of which equation (A-3) may be written as:

$$\frac{df}{dz'} = \mathbf{A}f \qquad \text{(A-11)}$$

where $\mathbf{A}$ is the coefficient matrix:

$$\mathbf{A} = \begin{bmatrix} 0 & 1 \\ -K_n & (1 - z')G' \end{bmatrix} \qquad \text{(A-12)}$$

The propagator matrix $\mathbf{P}$ is initialized as the unit matrix at $z' = 0$ and satisfies the same differential equation as f:

$$\frac{d\mathbf{P}}{dz'} = \mathbf{AP} \text{ ,} \qquad \text{(A-13)}$$

where:

$$f_i(z') = P_{ij}(z') f_j(0) = cP_{i2}(z') \qquad \text{(A-14)}$$

where c is an arbitrary constant. The boundary condition $\theta(0) = 0$ has been utilized on the far right-hand side of (A-14). The second boundary condition $\theta(1) = 0$ requires:

$$P_{12}(z' = 1) = 0 \qquad \text{(A-15)}$$

Equation (A-13) is solved for $\mathbf{P}(z')$ using a fourth-order Runge-Kutta-Gill procedure [14]; for a given value of G' a Newton-Raphson scheme is used to search for a value of K_n for which equation (A-15) is satisfied. Once K_n is determined both θ_n and $d_z\theta_n$ are automatically known to within an arbitrary constant as $P_{12}(z')$ and $P_{22}(z')$ respectively. ($d_z\theta_n$ is required to compute surface heat flow.)

In the limit as $G' \to 0$ equations (2), (A-2) and (A-3) take the form of thermal diffusion equations for which the eigenvalues are known to be $n^2\pi^2$, $n = 1, 2, \ldots$, and corresponding eigenfunctions are proportional to $\sin n\pi z'$. This fact allows an analytical check of the numerical scheme and enables us to locate all possible eigenvalues. A test case with $G' = 10^{-4}$ reproduces the diffusion results to five significant figures. For all $G' > 0$ values of K_n are greater than $n^2\pi^2$; the transient modes associated with advection decay more rapidly than those associated with diffusion. For $G' \leqslant 1.0, K_n \approx n^2\pi^2$; for $G' \geqslant 10, K_n \approx 2nG'$, with a smooth transition for $1.0 < G < 10$. Graphs of θ_n at $G' = 10$ and $G' = 100$ are shown in Fig. A-1.

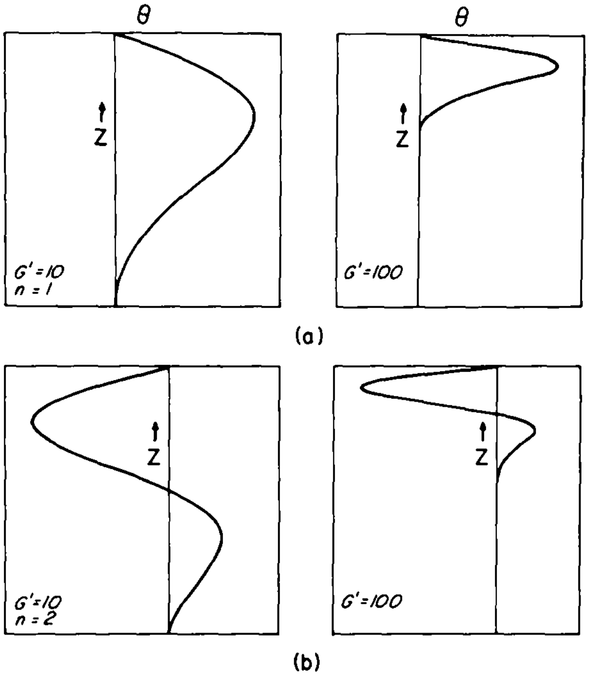

Fig. A-1. The first two eigenfunctions $\theta_n(z)$ for $G' = 10$ and $G' = 100$: (a) $n = 1$, (b) $n = 2$.

These show a departure from $\sin n\pi z'$ as G' increases. At large G' the largest amplitudes are concentrated upwards indicating the regions in which transient effects will persist the longest. As in all Sturm-Louiville problems the number of internal nodes in θ_n is $n - 1$.

Since there are an infinite number of K_n and θ_n which satisfy (A-3) we may write the general solution as:

$$T'(z', t') = \frac{-\mathrm{erf}[(z' - 1)\sqrt{G'/2}]}{\mathrm{erf}\sqrt{G'/2}} + \sum_{n=1}^{\infty} a_n \exp(-K_n t')\,\theta_n \qquad \text{(A-16)}$$

where a_n is the nth coefficient, to be determined from the initial conditions. At $t = 0$:

$$(1 - z') + \frac{\mathrm{erf}[(z' - 1)\sqrt{G'/2}]}{\mathrm{erf}\sqrt{G'/2}} = \sum_{n=1}^{\infty} a_n\theta_n \qquad \text{(A-17)}$$

Since the θ_n's are orthogonal with respect to $\exp[(z' - 1)^2\, G'/2]$ (equation (A-5)), multiplying both sides of (A-17) by $\theta_m \exp[(z' - 1)^2\, G'/2]$ and integrating over z' yields:

$$a_n = \left(\int_0^1 \left\{(1 - z') + \frac{\mathrm{erf}[(z' - 1)\sqrt{G'/2}]}{\mathrm{erf}\sqrt{G'/2}}\right\}\theta_n \times \exp[(z' - 1)^2\, G'/2]\, \mathrm{d}z'\right) \times \left(\int_0^1 \theta_n\theta_n \exp[(z' - 1)^2\, G'/2]\, \mathrm{d}z'\right)^{-1} \qquad \text{(A-18)}$$

where the right-hand side of (A-18) is known. The a_n are thus determined. Substituting (A-18) into (A-16) gives the dimensionless expression for the time-dependent solution of equation (2).

References

1 N.H. Sleep, Thermal effects of the formation of Atlantic continental margins by continental break up, Geophys. J.R. Astron. Soc. 24 (1971) 325.

2 W.F. Haxby, D.L. Turcotte and J.B. Bird, Thermal and mechanical evolution of the Michigan Basin, Tectonophysics 36 (1976) 57.

3 N.H. Sleep and N.S. Snell, Thermal contraction and flexure of mid-continent and Atlantic marginal basins, Geophys. J.R. Astron. Soc. 45 (1976) 125.

4 D.P. McKenzie, Active tectonics of the Alpide-Himalayan Belt: the Aegean Sea and surrounding regions, Geophys. J.R. Astron. Soc. 55 (1978) 217.

5 D.P. McKenzie, Some remarks on the development of sedimentary basins, Earth Planet. Sci. Lett. 40 (1978) 25.

6 J.M. Profett, Cenozoic geology of the Yerington district, Nevada, and implications for the nature and origin of Basin and Range faulting, Geol. Soc. Am. Bull. 88 (1977) 247.

7 O. de Charpal, P. Guennoc, L. Montadert and D.G. Roberts, Rifting, crustal attenuation and subsidence in the Bay of Biscay, Nature 275 (1978) 706.

8 J.G. Sclater, L. Royden, S. Semken, C. Burchfiel, L. Stegena and F. Horvath, The role of continental stretching in the Neogene subsidence of the Pannonian Basin, Earth Planet. Sci. Lett. (in press).

9 P. Christie and J.G. Sclater, Nature 283 (1980) 729.

10 B. Parsons and J.G. Sclater, An analysis of the variation of ocean floor bathymetry and heat flow with age, J. Geophys. Res. 82 (1977) 803.

11 M.S. Steckler and A.B. Watts, Subsidence of the Atlantic-type continental margin off New York, Earth Planet. Sci. Lett. 41 (1978) 1.

12 A.B. Watts and W.B.F. Ryan, Flexure of the lithosphere and continental margin basins, Tectonophysics 36 (1976) 25.

13 F. Gilbert and G.E. Backus, Propagator matrices in elastic wave and vibration problems, Geophys. 31 (1966) 326.

14 M.J. Romanelli, Runge-Kutta methods for the solution of ordinary differential equations, in: Mathematical Methods for Digital Computers, A. Ralston and H.S. Wilf, eds. (Wiley, New York, N.Y., 1960) 110.